Detection of Spread-F, foF2 values and Planetary and Gravity Wave Signatures using Digisonde instruments and their comparison with COSMIC-I/FORMOSAT-3, SAMI and IRI data

Bhaneja, P[(1)(3)], Bullett, T[(2)], Klenzing, J[(3)]

(1) Universities Space Research Association, Columbia, MD, USA;

(2) NCEI/National Oceanic and Atmospheric Administration, Boulder, CO, USA;

(3) ITM Physics Lab Goddard Space Flight Center, Greenbelt, MD, USA;

Corresponding Author: Preeti.Bhaneja@nasa.gov

ABSTRACT

A comprehensive statistical study of Spread F using digisonde data from low and midlatitude global sites has been conducted. Data from five midlatitude stations in the north-American include: Ramey AFB, Puerto Rico (18.5°N, 67.1°W, -14° declination angle) for 1996-2011, Wallops Island, Virginia (37.95°N, 75.5°W, -11° declination angle) for 1996-2011, Dyess, Texas (32.4°N, 99.8°W, 6.9° decl. angle) for 1996-2009, Boulder, Colorado (40°N, 105.3°W, 10° decl. angle) for 2004-2011, and Vandenberg AFB, California (34.8°N,120.5°W, 13° decl. angle) for 1996-2009. Low-latitude stations include: Ascension Island (7.9°S, 14.4°W, -15.09° decl. angle) from 2000-2014, Kwajalein (8.71°N, 167.7°E, 7.5° decl. angle) from 2004-2012. Multiple algorithms have been written to process the raw data and determine spread F by using edge detection and pattern recognition techniques. Pattern recognition algorithms are used to determine the presence of both range and frequency spread F. Algorithms have also been written to find foF2 and hmF2 values for obtaining the density profile of the ionosphere. Vertical Incidence Pulsed Ionospheric Radar (VIPIR) data was also processed for a few of these sites for determining the foF2 values and the comparison between the two instruments. Findings based on work carried out to date include:

- Determination of seasonal and solar cycle variation patterns.
- Correlation between digisonde, COSMIC-1/FORMOSAT-3 satellite data and SAMI and IRI models values to check for validity of data.
- Wave analysis has been performed to detect the presence of planetary and gravity wave type patterns in foF2 values with periods ranging from a few hours to a few days and for various seasons.

1. INTRODUCTION

Density irregularities in the ionosphere are often observed as a spread pattern in data from radio sounding techniques such as digisondes referred to as Spread F. Spread F is observed at both mid latitudes called Midlatitude Spread F (MSF) and equatorial latitudes called Equatorial Spread F (ESF); both are caused by different instability mechanisms due to the angle of the magnetic field relative to the ionospheric plasma layer. Ionospheric F region is known to exhibit anomalies and irregularities during both day and nighttime. Various anomalies have been observed in the ionospheric F2 region as observed in the critical frequency and the electron density values. Ionospheric irregularities are temporal and spatial variations of the electron density lasting from a few minutes to a several hours.

Planetary wave signatures (PWS) observed in the ionosphere occur either due to the planetary waves (PW) in the mesosphere-thermosphere (MLT) region or due to geomagnetic activity variations with observed wave periods of 2-3, 5-6, 10, 16, 23 and 35 days [*Altadill & Apostolov,* 2003]. These waves propagate towards the ionosphere creating wave oscillations as observed in the density observations. Atmospheric buoyancy waves or gravity waves are generated from a variety of sources, including thunderstorms [*Lay et al*., 2015] and auroral disturbances [*Nygren et al*., 2015]. Gravity waves are considered to be a seeding mechanism that creates density perturbations in the ionosphere leading to spread [*Lastovicka*, 2006;].

Spread-F is a nighttime phenomenon where the irregularities are observed on the ionograms which are plots of frequency vs. height obtained by reflections of the transmitted signal into the ionosphere when they match the plasma frequency [*Bhaneja et al*., 2009, 2018]. For equatorial spread F, the various irregularities or spread patterns may be associated with multiple types of plasma structures, such as plumes, patches, bubbles, and blobs [*Aarons*, 1993].

The data in O-Mode trace is used to generate ionograms for identifying spread F. Ionograms obtained during spread F events show thickness or spread in the F region trace that is significantly greater than that obtained for a normal ionosphere. ***Figure 1*** shows four ionograms indicating different conditions of the ionosphere. 1(a) indicates a quiet ionosphere, represented by a single trace. 1(b), (c) and (d) show ionograms with thick traces which implies strong spread conditions. The spread observed on the ionograms can be classified as range or frequency spread. **Range spread** refers to a condition in which there are multiple range echoes at a particular frequency. **Frequency spread** refers to the case in which multiple critical frequencies appear at fixed altitudes. Figures 1 (b), (c), (d) show range, range and frequency spread F and spread F in the form of a big blob respectively. The boxes shown are positioned by our autonomous edge detection software. Large pixel counts in box 1 correspond to range spreading (RS), and large pixel counts in box 2 correspond to frequency spreading (FS).

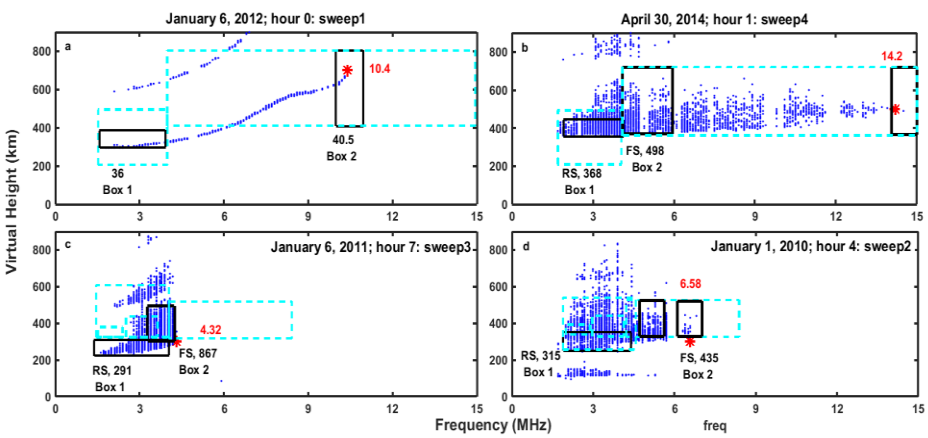

Figure 1- a) Non-spread F event. Different Spread F events; b) Range Spread F; c) Range and Frequency Spread F; d) Spread F in a form of a big blob. The dotted lines are the boundary boxes, and the solid line box is the box selected by the algorithm for determining Range (RS, Box 1) and Frequency (FS, Box 2) spread F for an individual ionogram. The corresponding numbers with RS and FS are the pixel counts in each box which determine the spread F. The red star and the corresponding number is the foF2 value determined for the individual ionogram.

2. OBSERVATIONS

Our dataset is comprised of nighttime ionograms at 15-minute intervals. **Figures 2-3** show the monthly plots with foF2 and both range and frequency spread F. The focus of this study is to determine statistics of spread F events (**Figures 7-8**), detect foF2 values and compare them with COSMIC measured, IRI and SAMI models generated values (**Figure 4**). **Figures 5-6** show the presence of planetary and gravity wave type patterns in foF2 values.

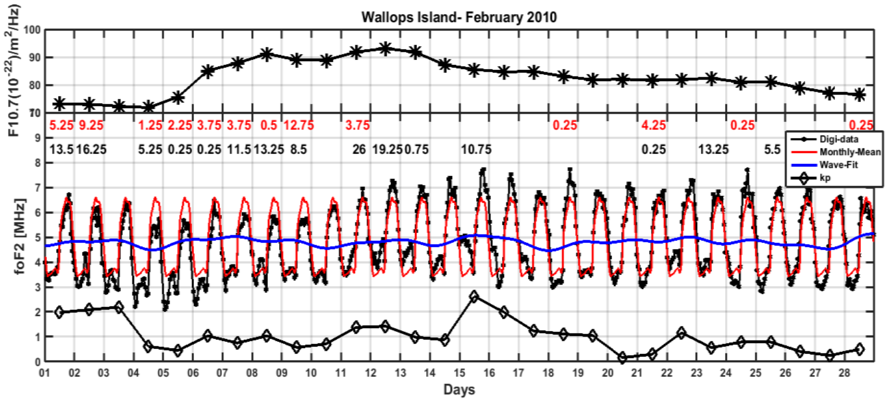

FIGURE 2 –VIPIR (Wallops Island) for February 2010. The numbers in red correspond to the duration hours of Range Spread F while the black correspond to Frequency Spread F. The top panel shows the F10.7 values and the lower curve with diamond symbols represents the kp values. The blue line is the wave fit with wave periods of 2,3,4,5 and 7 days for the foF2 values.

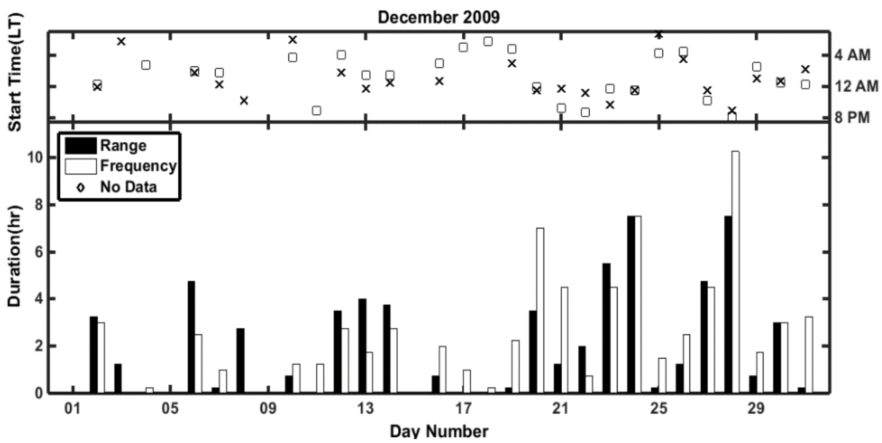

FIGURE 3 –Monthly occurrence plot for December 2009 showing range and frequency spread F onset time and duration for nighttime hours between 8PM-6AM LT. The cross symbol denotes the start time for range spread F and the square symbol denotes the start time for frequency spread F.

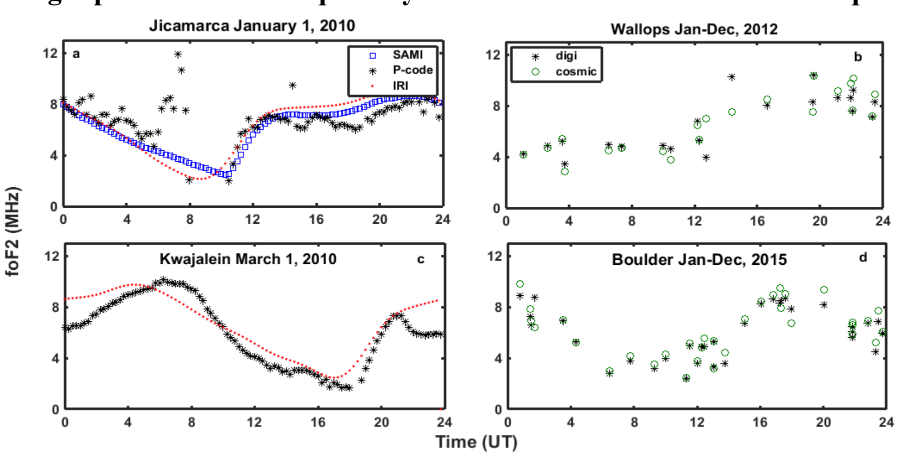

FIGURE 4 – Comparison of foF2 for digisonde data from Jicamarca, Wallops, Kwajalein & Boulder with COSMIC, SAMI and IRI values. The left hand side shows comparison with SAMI (blue squares) and IRI (red dots) models, while the right hand side shows comparison with COSMIC-1 (green circles) data. The black stars are the digisonde data for the different stations.

Figures 5-6 provide the amplitude spectra of the foF2 values using the Lomb-Scargle periodogram analysis. **Figure 5** shows the planetary and gravity type wave oscillations in the foF2 values detected from the ionograms. The foF2 values show planetary wave signatures of 2,3,4,5 and 8 days wave oscillations and also the presence of semi-durnal tides (12 hours) and teri-durnal tides (8 hours) and gravity wave signatures from 3 to 6 hours. **Figure 6** shows the wave period variation for the different seasons of spring, summer, fall & winter.

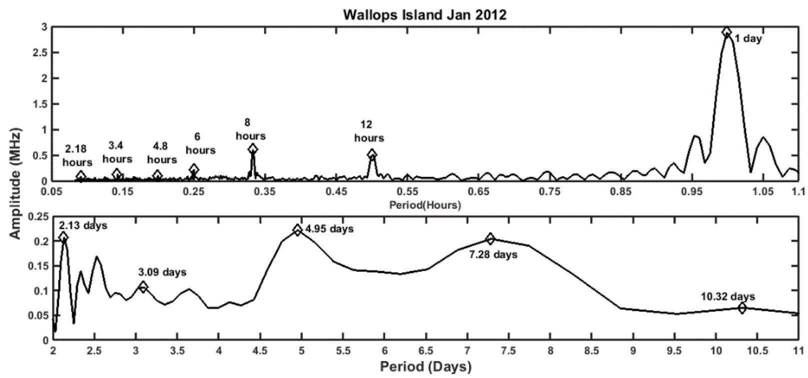

FIGURE 5 – Wave Analysis for foF2 values for Dec 2010. Amplitude spectra of digisonde data (Wallops Island) for Jan 2012 showing the peak periodicities in the foF2 data.

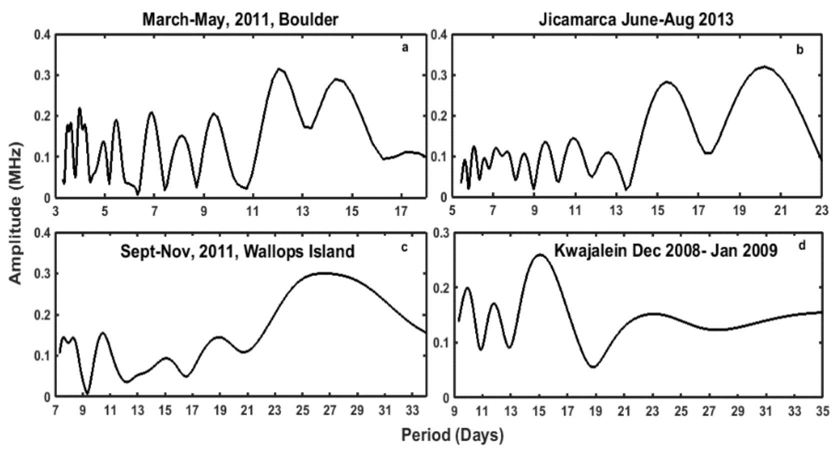

FIGURE 6- Wave periods and Amplitudes for foF2 from Wallops Island and Boulder stations obtained using Lomb-Scargle periodogram analysis for all the four seasons starting from (a) spring season, (b) summer season, (c) fall season, and (d) the winter season.

Figures 7 (left hand side) & 8 (right hand side) show the solar and seasonal cycle variations of both mid and low latitude regions. The blue line in the **Figure 8** is the angle between the dusk terminator and local magnetic field. More spread F during minimum angle indicates that efficient electric field mapping between conjugate hemispheres is important for the occurrence of spread F.

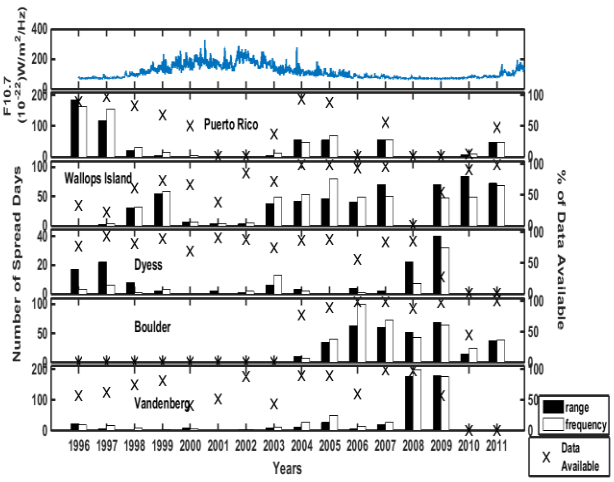

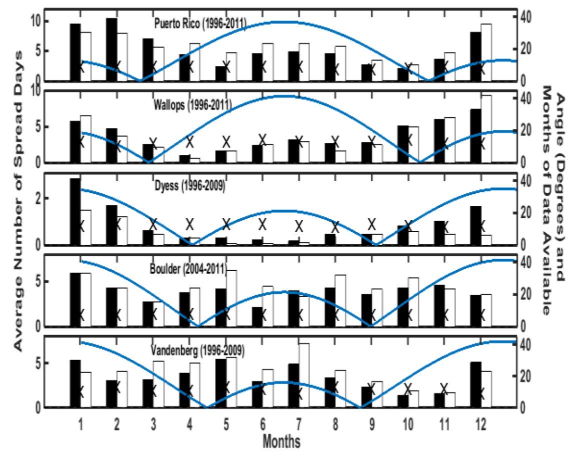

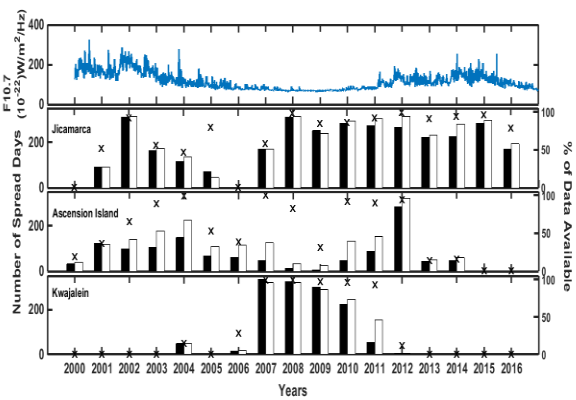

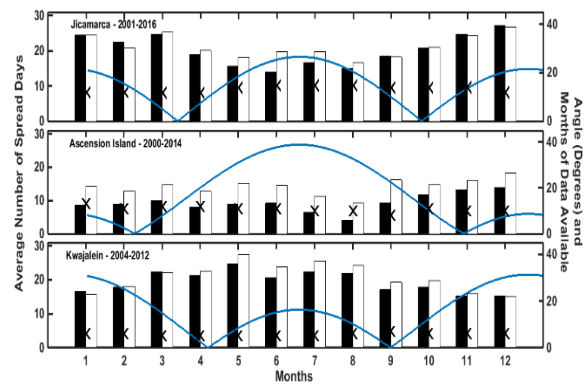

FIGURE 7 (left hand side) –Plots show the solar cycle variation of spread F for midlatitude sites; 16 years (1996-2011) of data for Wallops Island, Dyess, Vandenberg and Puerto Rico and 7 years (2004-2011) of data for Boulder; low latitude sites; 16 years (2001-2016) for Jicamarca, 15 years (2000-2014) for Ascension Island, and 9 years (2004-2012) for Kwajalein. The top panel shows the solar flux data which is higher during the solar maximum years (2000-2003 and 2012-2015).

FIGURE 8 (right hand side) – Plots shows the seasonal cycle variation for the sites for the available data. The left-hand side shows the average number of spread days and the months of data available. The right-hand side shows the angle between the declination and the terminator. The black bars represent range spread F while white bars represent frequency spread F and the blue line represents the angle.

3. CONCLUSIONS

Figure 1 shows the various kinds of spread events observed and the time-cycle of spread for low latitudes from huge plumes and intense spread (1b) to less intense spread (1d) to spread signatures as observed for mid latitude regions (1c). **Figures 2-3** show monthly plots of foF2 values and MSF events respectively. It is evident from **Figure 4** that the algorithm detects fairly accurate values of foF2 as shown for different stations with data validated by COSMIC satellite measured values and IRI and SAMI model values. **Figure 5** shows that the foF2 values have signatures of gravity waves from 3 to 6 hours, teri-durnal tides (8 hours), semi-durnal tides (12 hours) and planetary wave signatures from 2-5 and 8 days wave oscillations. The wave fit using these PW periods is also observed in **Figure 2**. These oscillations may be due to geomagnetic effects or terrestrial weather effects. **Figure 6** shows the variation of wave periods with different seasons. The spring season has wave periods starting at 4 days; the summer season has wave periods starting from 5 days; the fall season show waves from 8 days; and the winter season show waves from 10 days and up to 35 days for all these seasons. **Figure 7** shows the solar cycle variation. MSF occurrence rate and duration is higher during solar min than during solar max for all five stations. Equatorial Spread F doesn't have any particular solar cycle variation for the three sites. An interesting observation evident is that almost all stations experience more range spread F events during solar min, and more frequency spread F events during solar max. **Figure 8** shows seasonal variation. All the stations show different seasonal variations, presumably due to their varying longitudes, declinations, or localized forcing from lower altitude sources. The observations are summarized in **Table 1**. Midlatitude stations are in black and equatorial stations are in red color. An interesting observation is that places located at negative declination tend to have most spread F conditions during fall and winter seasons while places at positive declination have most spread F during spring and summer seasons.

Stations	Latitude	Longitude	Declination	Season with maximum MSF occurrences	Season with minimum MSF occurrences
Puerto Rico	18.5	67.1	-14°	Winter solstice	Spring equinox, Vernal equinox
Wallops Island, Virginia	37.95°	75.5°	-11°	Vernal equinox, winter solstice	Spring equinox, Summer
Dyess, Texas	32.4°	99.8°	6.9°	Winter solstice	Spring, Summer, Vernal Equinox
Boulder, Colorado	40°	105.3°	10°	Early summer, autumn equinox	Spring Equinox, Winter
Vandenberg, California	34.8°	120.5°	13°	Summer solstice, winter solstice	Fall
Jicamarca, Peru	12°S	76.8°W	-2.5°	Fall and winter	Spring and Summer
Ascension Island	7.9 S	14.4W	-15.09	Fall and December	Summer
Kwajalein	8.71°N	167.7° E	7.5°	Spring and summer	Fall and winter

REFERENCES

1. Aarons, J., *Space Science Reviews*, 63, 209-243, 1993.
2. Altadill, D., and Apostolov, E.M., *J. Geophys. Res.*, 108, A11, 1403, doi:10.1029/2003JA010015, 2003.
3. Bhaneja, P., et al., *J. Atm. Solar-Terres. Phys.*, 167, 146-155, doi.org/10.1016/j.jastp.2017.11.016, 2018.
4. Bhaneja, P., et al., *J. Geophys. Res.,* 114, A04301, doi:10.1029/2008JA013212, 2009.
5. Lay, E. H., et al., *J. Geophys. Res.*, 10.1002/2015JA021334, 2015.
6. Nygrén, T., et al., *J. Geophys. Res.*, 120, 3949–3960. doi:10.1002/2014JA020794, 2015.
7. Lastovicka, J., *J.Atmos. Solar-Terres. Physics*, 68, 479-497, 2006.

ACKNOWLEDGMENTS

The data for all the plots have been provided by NGDC, SPIDR, SPDF, IRI and SAMI.